Packing polymorphism of α-helices in a synthetic polypeptide

S. Sasaki
Department of Polymer Chemistry, Tokyo Institute of Technology, Ookayama, Meguro-ku, Tokyo, 152 Japan
(Received 3 October 1985; revised 11 November 1985)

The manner of packing of α-helices in poly(δ-*N*-carbobenzoxy L-ornithine) films was studied by X-ray diffraction. In addition to the (pseudo)hexagonal (type I) and the tetragonal (type II) forms, a new, monoclinic form (type III) was found. The electron density projection along the chain axis was calculated for types I and II by means of Fourier synthesis. In the (pseudo)hexagonal unit cell of type I containing two helices, there is a helix-free space filled with side chains. Urethane groups of the side chains possibly form the intermolecular hydrogen bonds in type I, while the association is intramolecular in type II. Side chains are well incorporated into the crystalline order in type III. The structures are discussed in terms of interactions between interpenetrating side chains.

(Keywords: α-helix; packing; crystal modification; X-ray diffraction)

INTRODUCTION

Two crystal modifications are known for α-helical poly(δ-*N*-carbobenzoxy L-ornithine) (PCLO)[1,2]

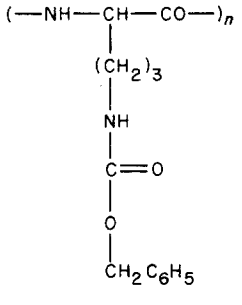

The molecular chain assumes the right-handed α-helical conformation, and the glass-like transition temperature associated with the onset of the side-chain motion in the solid state is about 30°C.[2] In films as cast from chloroform or dioxane (type I), the two-dimensional unit cell in the projection along the chain axis is pseudohexagonal with dimensions $a \sim b \sim 23$ Å, and conatins two helices (the number of helices passing through a unit cell, $N = 2$). The crystallinity is poor. The slight lattice distortion ($\gamma = 119.5°$) from the hexagonal unit cell was observed by inspecting X-ray reflections for the as-cast film with uniplanar orientation. Such a small distortion, however, could not be detected for the uniaxially oriented film, for which equatorial reflections overlapped and the mean spacings were explained by a hexagonal unit cell with dimension $a = 22.8$ Å. Accordingly, $\gamma = 120°$ is assumed in this work.

Type I is irreversibly transformed into a highly crystalline form (type II) at about 140°C.[2] In type II, the two-dimensional unit cell is tetragonal with dimension $a = 14.7$ Å, and contains one α-helix ($N = 1$). As will be discussed below, the molecular and crystal structure is crystallographically tetragonal.

In addition to types I and II, type III was found incidentally, the packing being slightly distorted from that of type II. The cross sections of the unit cells of types II and III are about one half that of type I.

The most common arrangement of α-helices in the crystalline phase is hexagonal close packing (*Figure 1a*)[3,4]. Slight distortions from the hexagonal lattice have often been observed and attributed to the alternating arrangement of helices pointing up and down[5-7]. In a modification of poly(γ-benzyl L-glutamate) (PBLG), seven α-helices form an asymmetric unit in the large hexagonal unit cell indicated by the broken lines in *Figure 1a*[8]. These modifications may be classified as hexagonal. Secondly, tetragonal packing (*Figure 1b*), like type II of PCLO, has been observed for a few cases[9,10]. In PCLO, about half the side chains are associated via hydrogen bonds at room temperature[2]. Such interactions may be responsible for the manner of packing. On the other hand, the hexagonal unit cell with $N = 2$, like type I of PCLO, has been found for poly(β-phenethyl L-aspartate)[11], copoly(γ-methyl, hexyl L-glutamate)s[12], and poly(γ-*n*-dodecyl L-glutamate)[13]. The manner of arrangement of two helices in the hexagonal unit cell has not been clear.

In this paper, the structures of type I and II of PCLO are analysed in the equatorial projection by Fourier synthesis. The X-ray data of type III were good enough to determine the helical parameters, but not appropriate for the Fourier analysis because of reflection overlapping.

EXPERIMENTAL

PCLO was synthesized by the *N*-carboxyanhydride method, and identified by elemental analysis and its n.m.r. spectra[2]. The molecular weight was estimated to be about 1.7×10^5 from the intrinsic viscosity.

The concentrated solution in chloroform was observed under a microscope to form a cholesteric liquid crystal. Generally, liquid crystalline clusters in solutions of

0032-3861/86/060849-07$03.00

polypeptides are aligned in the electric-field direction. Well oriented specimens of type I were prepared by evaporating the solvent between two electrodes under an electric field of 1 kV cm^{-1}. The films were dried *in vacuo* for several days. The X-ray diffraction pattern was essentially equivalent to that of the film prepared by stroking the concentrated solution onto a glass plate.

X-ray diffraction measurements with Ni-filtered Cu Kα radiation were made by using a cylindrical camera. Reflection spacings were calibrated against reflections of silicon powder sprinkled over the specimen. Reflection intensities were measured from the photographs by using a microphotometer, and corrected for the Lorentz polarization factor.

The β pleated-sheet structure was formed in PCLO films kept at room temperature for a few years[14]. Such films were insoluble in chloroform. The film after extraction with chloroform gave the diffraction pattern and infra-red spectra characteristic of the β-structure. The intersheet spacing was 25 Å, and the interchain distance in the plane of the sheet was 4.6 Å.

RESULTS AND DISCUSSION

Formation of three modifications

Uniaxially oriented films of type II were prepared by annealing oriented films of type I at 150°C for 20 min, where the weight loss was not observed. Films of type III were obtained by standing films of type II at room temperature for a few months. Type III was reversed to type II by heating up to 150°C. Dissolution and recasting of films of types II and III gave the film of type I. The transition from type II to type I did not take place in the solid state. It was observed when the film of type II was allowed to absorb solvent vapour and then dried. The films of types II and III were highly crystalline, while the crystallinity of type I was invariably poor.

The X-ray fibre patterns of the oriented films are shown in *Figure 2*. The parameters of the two-dimensional unit cells determined from the spacings of the equatorial reflections are listed in *Table 1*. The meridional reflection corresponding to the unit height p was observed by tilting oriented films by *ca.* 30° from the normal to the X-ray beam (*Figure 3*). It appears at $1.49_3 \pm 0.002$ Å for type I, and at 1.500 ± 0.002 Å for types II and III. Because of nematic disorder, the true unit height of type I should be larger than the apparent value. Since the backbone conformation is regarded to be essentially the same, the packing polymorphism may be attributed to side-chain behaviour.

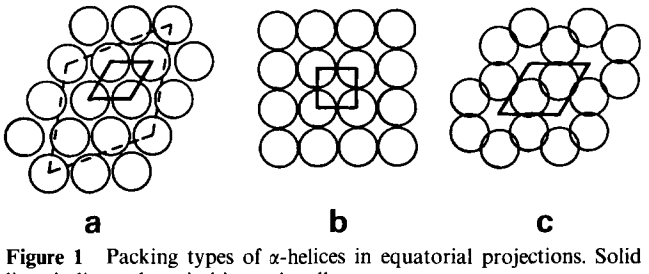

Figure 1 Packing types of α-helices in equatorial projections. Solid lines indicate the primitive unit cell

Structure of type I

Crystallographically, two helices conforming with the hexagonal unit cell are uniquely located at $(x, y) = (2/3, 1/3)$ and $(1/3, 2/3)$ (*Figure 1c*). This packing is rather peculiar; one open space exists per two helices. However, the structure is not so irrational if the associated side chains fill up the space.

Before the analysis based on this model, other possibilities were examined. First, the arrangement of two helices at $(x, y) = (0, 0)$ and $(0, 0.5)$ was considered. In this case, the hexagonal symmetry is abolished; the unit cell is reduced to the half-size orthorhombic cell ($N = 1$) with dimensions given by $a/3^{\frac{1}{2}} = b = 22.8/2$ Å. In fact, such a deformed lattice with particular dimensions is unlikely. Secondly, the two-stranded coiled-coil conformation was suspected. A three-stranded coiled-coil structure was once proposed for the complex phase of PBLG with dimethylformamide[15]. The features of the diffraction pattern were similar to those expected for a coiled coil according to diffraction theory[16]. Parry and Elliott, however, indicated that those features come from the quasihelical association of side chains[17]. (In their model, three straight α-helices pass through in the hexagonal unit cell. It was suggested later that four helices are contained in the unit cell[13,18].) The pitch angle ψ of the major helix of a coiled coil has been supposed to be 10–15°, and the

Table 1 Two-dimensional lattice parameters in PCLO films

Packing type	Lattice parameters[a]
Type I	hexagonal, $a = 22.8$ Å, $p = 1.49_3$ Å, $N = 2$, $\rho_c = 1.22$
Type II	tetragonal, $a = 14.7$ Å, $p = 1.50$ Å, $N = 1$, $\rho_c = 1.27$ (true unit cell: tetragonal, $a = 20.8$ Å, $c = 60.00$ Å, $N = 2$)
Type III	monoclinic, $a = b = 14.7_5$ Å, $\gamma = 97°$, $p = 1.50$ Å, $N = 1$, $\rho_c = 1.27$ (true unit cell: orthorhombic, $a = 22.0_9$ Å, $b = 19.9_5$ Å, $c = 60.00$ Å, $N = 2$)

[a] p, unit height; N, number of helices passing through the unit cell; ρ_c, calculated density in units of grams per cubic centimetre

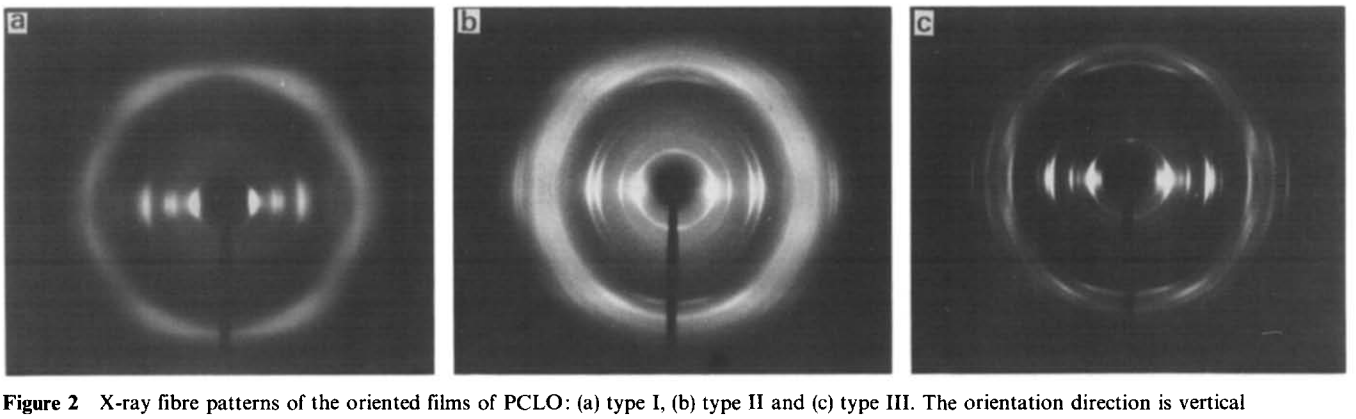

Figure 2 X-ray fibre patterns of the oriented films of PCLO: (a) type I, (b) type II and (c) type III. The orientation direction is vertical

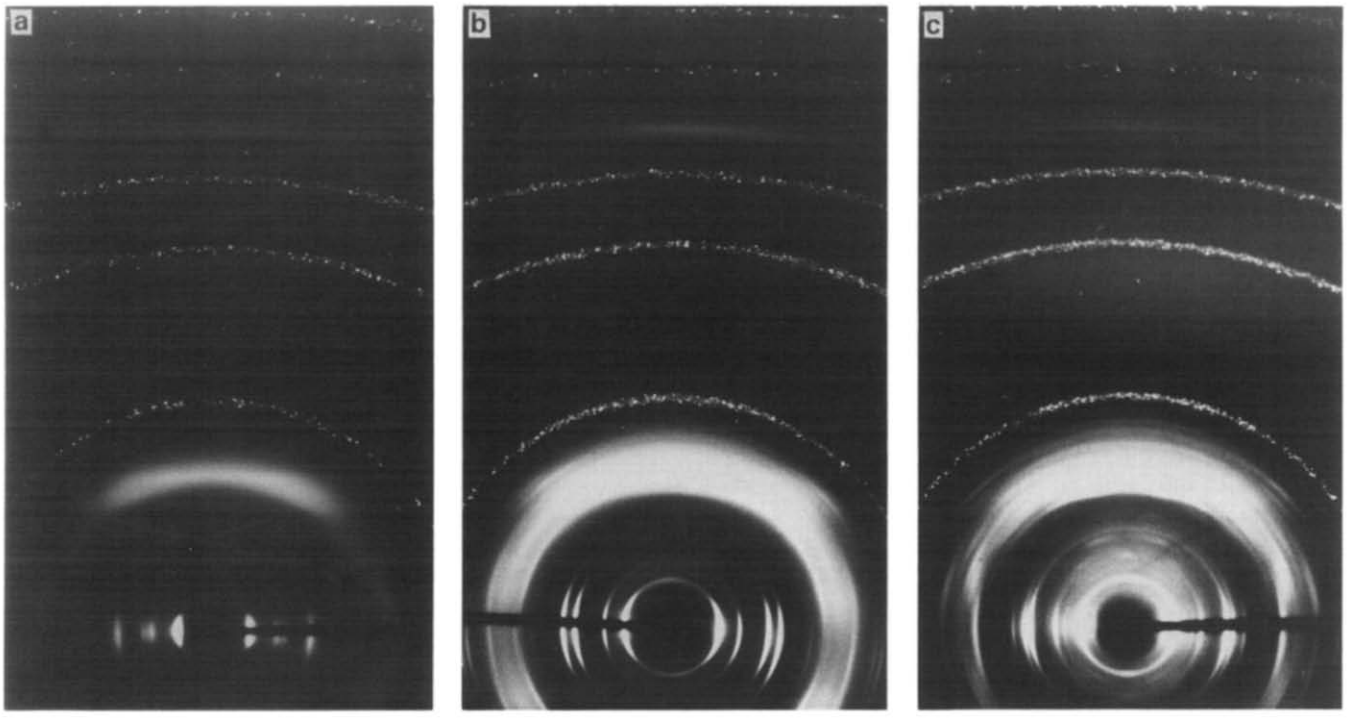

Figure 3 X-ray diffraction patterns taken by tilting the oriented films of PCLO from the normal to the beam: (a) type I, (b) type II and (c) type III. The 1.5 Å meridional reflection appears between the 3 1 1 and 4 0 0 reflections of silicon powder

meridional reflection corresponding to the average unit height is expected to appear at $1.50\ \text{Å} \times \cos\psi = 1.48 - 1.45\ \text{Å}$[16,17]. However, the complex phase of PBLG exhibited the strong meridional reflection at 1.50 Å[17]. For type I of PCLO, Del Pra *et al.*[1] reported that a meridional reflection appeared at 1.47 Å. However, it was observed at 1.49_3 Å for our oriented films of type I. Furthermore, the film of type I showed the infrared spectrum exactly identical to that of type II, which assumes the straight α-helical conformation. Even though the deformation of the straight helix to form the coiled-coil conformation is small, the spectrum should be changed somehow. The coiled coil was thus excluded.

Based on the two-chain hexagonal unit cell (*Figure 1c*), the structure was analysed. The electron-density projection along the chain axis can be determined by Fourier synthesis in the equatorial plane. The data of resolution 3.3 Å (*Table 2*) may be enough to determine the rough electron-density distribution. In the equatorial projection, the structure is probably centrosymmetric and may have diad axes lying in the plane; the structure factors are real, and assume the same values for pairs of $hk0$ and $kh0$ reflections.

The electron density projection at (x, y) is defined by the average of the density (x, y, z) along the z-axis over a repeat distance of c (assumed to contain 18 residues):

$$\rho(x,y) \equiv \frac{1}{c}\int_{z=0}^{c} \rho(x,y,z)\mathrm{d}z = \frac{18}{V}\sum_{h,k} F(h,k,0)\cos\{2\pi(hx+ky)\} \quad (1)$$

where V is the unit-cell volume and $F(h,k,0)$ is the structure factor (scaled per residue) of $hk0$ reflection. The structure amplitude $|F(h,k,0)|$ in a relative scale is determined from the intensity data by taking into account the multiplicity of the reflection. The only factor that cannot be determined from experiment is the sign of each structure factor. The phase factors (+1 or −1) were determined from the comparison between the observed data of $|F|$ and the molecular structure factors F_M calculated for various molecular models with possible side-chain conformations. Although the α-helix of PCLO does not have the 18-fold symmetry in the crystal lattice as mentioned below, the standard α-helical conformation is good enough for the calculation of F_M.

Table 2 X-ray equatorial data for type I of PCLO

Refl. no.	h	k	l	d_{calc} (Å)[a]	d_{obs} (Å)	I[b]	F	P	Sign of F_M
1	1	0	0	19.75	19.7	1.00	−25.5	−1	+
2	1	1	0	11.40	11.5	0.24	12.5	2	+
3	2	0	0	9.87	~10	0.26	−13.0	−1	+
4	2	1	0	7.46	7.4_7	0.74	−15.5	−1	+
5	3	0	0	6.58	~6.6	0.22	12.0	2	+
6	2	2	0	5.70	~5.6	0.18	8.8[c]	2	+
	3	1	0	5.48			−4.4[c]	−1	+
7	4	0	0	4.94	4.9_5	0.04	5.2	−1	−
8	4	1	0	4.31	4.3_1	0.24	−8.9	2	−
9	3	3	0	3.80	3.7_8	0.17	−8.4[c]	2	−
	4	2	0	3.73			4.2[c]	−1	−
10	6	0	0	3.29	3.2_9	0.13	−9.2	2	−

[a] Calculated spacings based on the unit-cell dimensions cited in *Table 1*
[b] Relative intensity data
[c] The same F_M value was assumed for the overlapped reflections

The structure factor of $hk0$ reflections is approximated by

$$F(h,k,0) = P(h,k,0)F_M(h,k,0) \quad (2)$$

where

$$P(h,k,0) = \sum_{j=1,2} \exp\{2\pi i(hx_j + ky_j)\} \quad (3)$$

is the interference factor due to the existence of two helices in the unit cell at $(x_1, y_1)=(2/3, 1/3)$ and $(x_2, y_2)=(1/3, 2/3)$. The P values are listed in the seventh column of *Table 2*. $F_M(h, k, 0)$ is the value of the molecular structure factor $F_M(R)$ at the radial co-ordinate R corresponding to the reciprocal-lattice point with indices $hk0$. The observed data of $|F|$ divided by P are compared with $F_M(R)$. The $F_M(R)$ (per residue) for the uniform α-helix is approximated by

$$F_M(R)=\sum_j f_j J_0(2\pi R r_j)\exp(-B_j R^2/4) \qquad (4)$$

where J_0 is the zero-order Bessel function, f_j is the atomic scattering factor, r_j is the distance from the helix axis, and B_j is the temperature factor of the jth atom in a residue.

Molecular models were built with standard bond lengths and bond angles. By calculation according to equation (4), the contribution from the hydrogen atoms was neglected, and appropriate B_j values were used by referring to the case of PBLG[19]. The $F_M(R)$ curves calculated for models 1 and 2 with the side-chain conformations illustrated in *Figure 4a* are shown in *Figure 5*. In models 1 and 2, the radial distance r_p of phenyl groups from the helix axis is about 9 Å. The lengths of vertical rods in *Figure 5* correspond to the observed data (after an appropriate scaling) expressed in the form of $|F/P|$. The $F_M(R)$ curves are in rather good agreement with the observed data. Since $F_M(R)$ given by equation (4) depends only on the r_j parameters, it is difficult to determine the side-chain conformation only from this comparison. However, the models with $r_p \leqslant 7.5$ Å gave small $F_M(R)$ values at $R \sim 0.12$ Å^{-1}, where $F_M(R)$ should be large. No other models could explain the observed data. Some discrepancies are unavoidable, since the side chains are expected to exist in disorder in several stable conformations. Models 1 and 2 should be considered as examples of such ideal conformations. From comparison in *Figure 5*, the phase factors of most reflections could be determined (given by the sign of $P \times F_M$). However, the phase factors of three reflections (nos. 2, 6 and 7 at $R=d^{-1}=0.09$, 0.18 and 0.20 Å^{-1}, respectively) were ambiguous. Then, electron-density maps were calculated for possible sets of phase factors. For Fourier synthesis according to equation (1), $F(0,0,0)=\Sigma f_j=264$ was included. The features of the calculated maps were similar. In some of them, the helix core was too deformed from the circular shape, while in others, the electron density in the side-chain region was impossibly high in comparison with that in the core region. A reasonable map could be easily chosen, and is shown in *Figure 6a*. The final set for F is given in *Table 2*.

An interpretation of the map is shown in *Figure 6b*. The region A is actually not vacant and some side chains make up this space, although the very small area with negative density appears numerically near the origin. In region B, there are double maxima with $\rho \sim 0.45$e Å^{-3}, the distances from the helix axis being about 7 and 9 Å, which may correspond to phenyl groups. The models with $r_p \sim 9$ Å, such as models 1 and 2, are preferable, since the models with $r_p \sim 7$ Å did not explain the intensity data. As illustrated in *Figure 6b*, the side chains are interpenetrated between neighbouring helices, and hydrogen bonds may be formed in region C.

Structure of type II

The sharp equatorial reflections (*Figure 2b*) indicate the regular tetragonal array of α-helices with $a=14.7$ Å (*Table 1*). In a previous paper[2], the true unit cell was suggested to be a double-size orthorhombic one ($N=2$) with dimensions $a=14.7$ Å $\times 2$ and $b=a/2$, resulting from the alternating arrangement of helices pointing up and down.

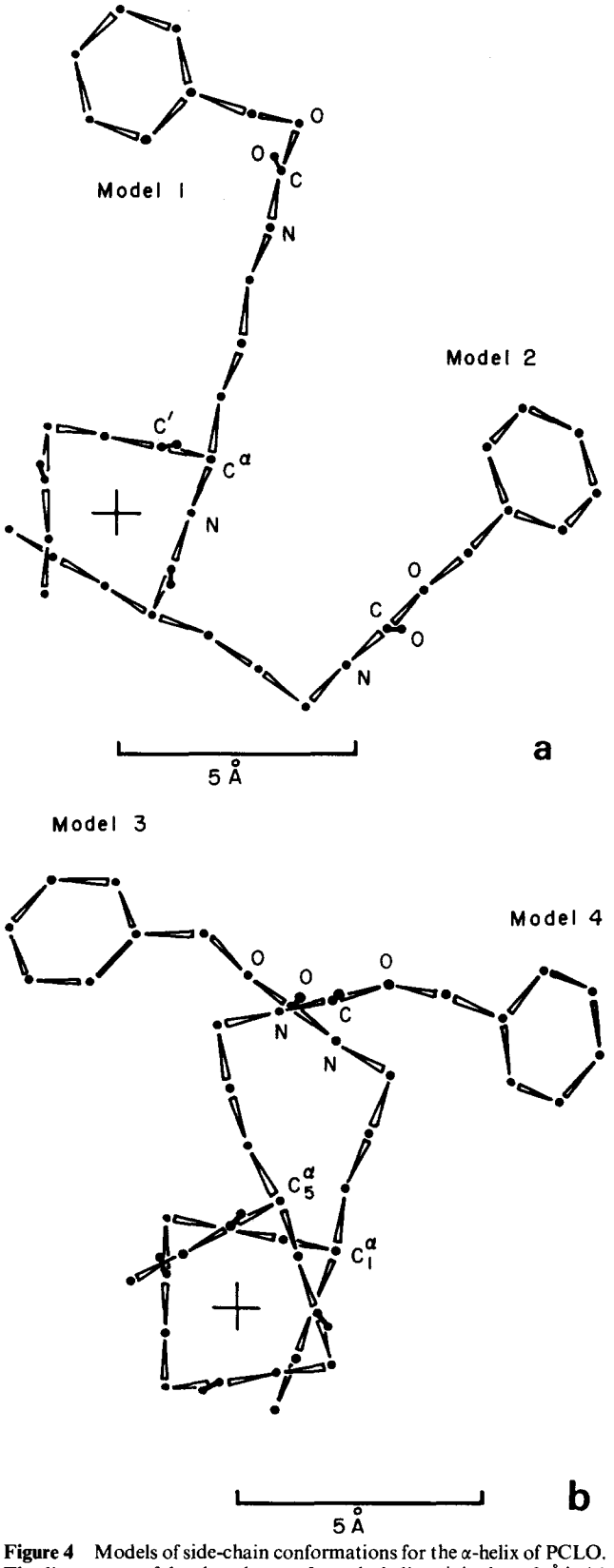

Figure 4 Models of side-chain conformations for the α-helix of PCLO. The distance, r_p, of the phenyl group from the helix axis is about 9 Å in (a) models 1 and 2, while about 8.3 Å in (b) models 3 and 4

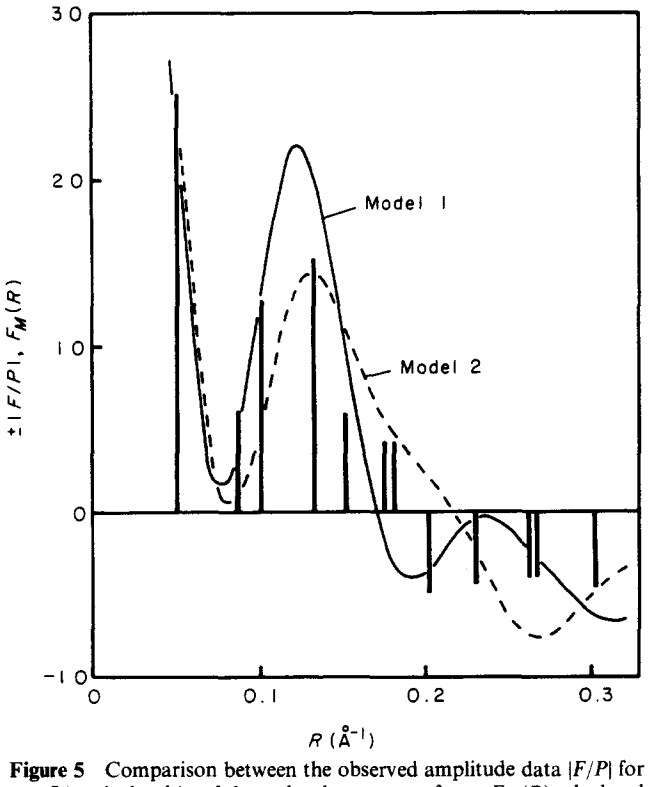

Figure 5 Comparison between the observed amplitude data $|F/P|$ for type I (vertical rods) and the molecular structure factor $F_M(R)$ calculated for models 1 and 2

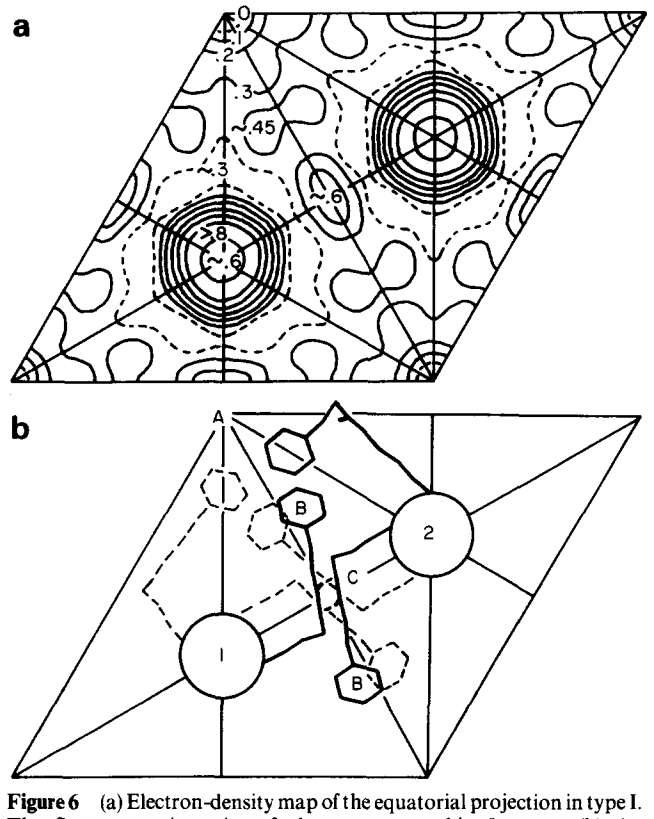

Figure 6 (a) Electron-density map of the equatorial projection in type I. The figures are in units of electrons per cubic ångstrom. (b) An interpretation of map (a)

However, this was not true. The electrically oriented film used in this work exhibited a diffraction pattern, in which the reflections are well resolved and a few are different from those of the shear oriented film. The spacings were explained by a tetragonal unit cell ($N=2$) with dimensions $a=14.7$ Å $\times 2^{\frac{1}{2}}=20.8$ Å and $c=1.50\times 40=60.00$ Å (*Table 1*). The molecular conformation has 40 residues per 11 turns (40/11 helix), so that the structure is crystallographically tetragonal. Reflections of type II are observed only on the layer lines that are expected to be strong from diffraction theory, and diffuse streaks overlap with Bragg reflections on the non-equatorial layer lines. In type III (transformed from type II in the solid state), many sharp reflections appear and diffuse streaks are much diminished. From comparison of these features, the side-chain region is considered to be less ordered in type II than in type III.

There is no difference in the features of the equatorial layer line between electrically oriented films and shear oriented ones. The equatorial data of structure amplitudes are given in *Table 3*. The two-dimensional structure of type II is probably centrosymmetric in the same way as in type I. The absence of the 3 0 0 reflection indicates that the molecular structure factor $F_M(R)$ crosses zero at $R\sim 0.20$ Å^{-1}. Only the models with $r_p=8$–8.5 Å, for example models 3 and 4 drawn in *Figure 4b*, satisfied this condition (*Figure 7*). Since one helix passes through the two-dimensional unit cell, the interference factor $P=1$ in equation (2), and the observed data of $|F|$ are directly compared with $F_M(R)$. The sign of $F_M(R)$, and therefore that of F, is negative in the range $R>0.20$ Å^{-1} and positive in the range $R<0.20$ Å^{-1} except for the 1 1 0 reflection. Near $R=0.1$ Å^{-1}, where the 1 1 0 reflection appears, $F_M(R)$ is very small. This discrepancy will be elucidated below.

The electron-density projection was calculated from equation (1) for two cases where the phase factor of $F(1,1,0)$ is $+1$ and -1. The features of the two maps were very similar: the density maxima due to side chains appear between neighbouring helices, as shown in *Figure 8*. For $F(1,1,0)>0$, the density integrated over the core region was too high by comparison with that over the side-chain region. The density concentration due to side chains in *Figure 8* gives a large negative contribution to $F(1,1,0)$. Therefore, the phase factor of $F(1,1,0)$ is -1. It is easily shown that the discrepancies in *Figure 7* between $|F|$ and $F_M(R)$ can be explained by the density concentration at $(x,y)=(\pm 0.42, \pm 0.06)$ and $(\pm 0.06, \pm 0.42)$. The final set for F is given in *Table 3*.

Table 3 X-ray equatorial data for type II of PCLO

Refl. no.	h	k	l[a]	R (Å^{-1})[b]	I[c]	F
1	1	0	0	0.068	1.00	24.8
2	1	1	0	0.096	0.14	−9.3
3	2	0	0	0.136	0.50	17.5
4	2	1	0	0.152	0.54	12.9
5	2	2	0	0.192	0.02	3.5
–	3	0	0	0.204	–	–
6	3	1	0	0.215	0.03	−3.0
7	3	2	0	0.245	0.07	−4.6
8	4	0	0	0.272	0.13	−9.0
9	4	1	0	0.280	0.22	−8.2
10	3	3	0	0.289	0.06	−6.0
11	4	2	0	0.304	0.11	−5.9
12	5	0	0	0.340	0.06	−2.0[d]
	4	3	0	0.340		−4.0[d]

[a] Indexing is based on the tetragonal unit cell ($N=1$) with dimension $a=14.7$ Å
[b] $R=d^{-1}$
[c] Relative intensity data
[d] $|F(5,0,0)|=(1/2)|F(4,3,0)|$ was assumed by taking into account the contribution from the density concentration due to side chains

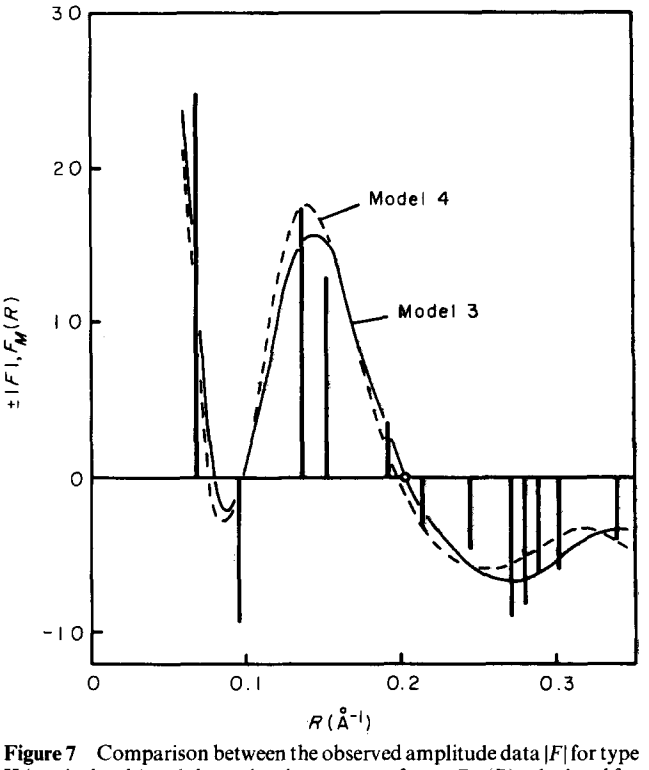

Figure 7 Comparison between the observed amplitude data $|F|$ for type II (vertical rods) and the molecular structure factor $F_M(R)$ calculated for models 3 and 4

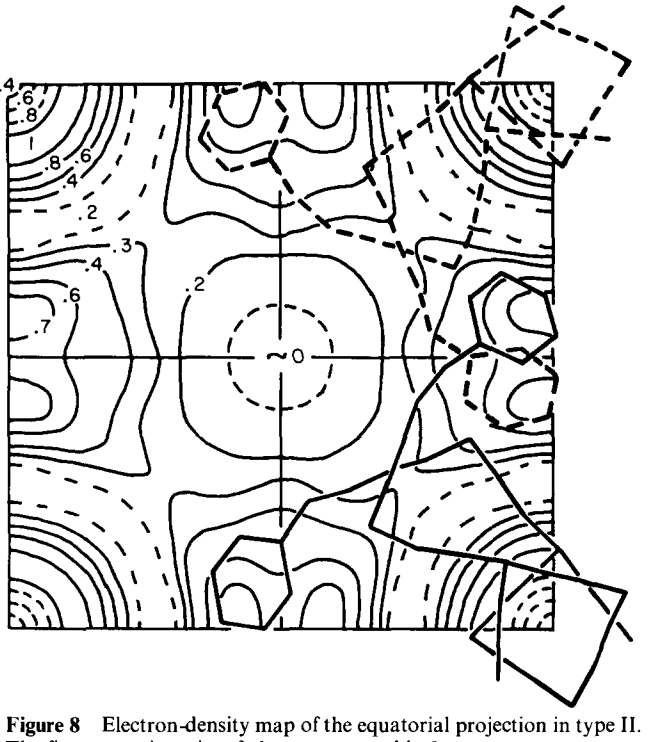

Figure 8 Electron-density map of the equatorial projection in type II. The figures are in units of electrons per cubic ångstrom

For the formation of intermolecular hydrogen bonds, side chains are required to extend so that the urethane groups can be associated. However, such models could not explain the intensity data. In models 3 and 4, the distance of the urethane group from the helix axis, about 6 Å, is too short to form the intermolecular hydrogen bonds, although the phenyl groups are interpenetrated between helices. Therefore, the hydrogen bonds in type II are formed within a molecule. Models 3 and 4 are such an ideal pair: the side chains attached to the ith and $(i+4)$th residues form intramolecular hydrogen bonds. These can be fitted to the density distribution, as shown in *Figure 8*. Naturally, not all the side chains orient in this way.

Structure of type III

The spacings of 16 equatorial reflections of type III were indexed by a monoclinic unit cell with dimensions

Table 4 Reflection spacings for type III of PCLO

Refl. no.	h	k	l[a]	d_{calc} (Å)[a]	d_{obs} (Å)	I[b]
1	1	1	0	14.64	14.6	vs
2	2	0	0	11.05	11.1	w
3	0	2	0	9.78	9.76	m
4	2	2	0	7.32	7.31	s
5	3	1	0	6.89	6.89	m
6	1	3	0	6.25	6.25	m
7	4	2	0	4.81	4.82	m
8	2	4	0	4.47	~4.4	vw
	5	1	0	4.31		
9	1	5	0	3.85	3.84	vw
10	6	0	0	3.68	3.66	m
	5	3	0	3.66		
	4	4	0	3.66		
11	6	2	0	3.45	3.44	w
	3	5	0	3.45		
12	2	6	0	3.13	3.13	vw
	7	1	0	3.12		
13	6	4	0	2.94	2.94	vw
	5	5	0	2.93		
14	1	7	0	2.77	2.77	vw
	8	0	0	2.76		
15	8	2	0	2.66	2.64	vw
	3	7	0	2.61		
16	9	1	0	2.44	2.42	vw
	8	4	0	2.40		
	2	8	0	2.39		
17	0	0	4	15.00	15.0	m
18	0	1	4	11.90	11.9	vw
19	4	2	4	4.58	4.58	w
20	4	3	4	4.06	4.03	w
21	1	1	5	9.28	~9.3	vw
22	2	3	5	5.08	5.06	vw
23	1	4	5	4.43	4.43	m
24	0	0	6	10.00	10.0	w
25	1	0	7	7.99	~7.9	w
	0	1	7	7.85		
26	0	4	7	4.25	~4.2	w
	3	3	7	4.24		
	4	2	7	4.19		
27	3	1	8	5.07	5.08	vw
28	1	3	8	4.80	4.82	w
29	1	0	9	6.38	6.37	vw
30	0	2	9	5.51	5.52	vw
31	3	3	10	3.79	3.80	w
	0	4	10	3.79		
32	1	0	11	5.30	5.30	w
33	1	1	11	5.11	5.13	m
34	2	0	11	4.89	4.90	w
35	1	2	11	4.66	4.66	m
36	3	0	11	4.38	4.39	w
37	1	3	11	4.11	4.13	2
38	3	3	11	3.64	3.63	w
	0	4	11	3.64		
	4	2	11	3.61		
39	0	2	12	4.45	4.46	w
40	1	0	14	4.21	4.23	w
41	1	0	15	3.94	3.94	w
42	1	0	16	3.70	3.70	w
43	1	0	17	3.49	3.50	w
44	0	0	40	1.50	1.50	m

[a] Indexing and calculation are based on the true unit cell ($N=2$) with dimensions cited in *Table 1*

[b] Visual intensity data: vs = very strong, s = strong, m = moderate, w = weak, vw = very weak

$a=b=14.7_5$ Å and $\gamma=97°$ ($N=1$). However, many non-equatorial reflections suggest that the true unit cell is a double-size orthorhombic one ($N=2$) with dimensions $a=22.0_9$ Å and $b=19.9_5$ Å (*Tables 1* and *4*). Meridional reflections appear at 15.0, 10.0 and 1.50 Å. The strong layer line associated with the helix pitch corresponds to the eleventh layer line. Therefore, the molecular conformation is similar to that of type II, which is described by 40/11 helix. However, the presence of meridional reflections at 15.0 and 10.0 Å (indexed to 004 and 006 reflections, respectively) indicates that the molecule including the side chains has crystallographically only the twofold screw symmetry (20 residues in an asymmetric unit). Reflections from independent reciprocal-lattice points are overlapped for several equatorial spots. The Fourier analysis was then given up in spite of the well-defined data.

The infra-red spectrum of type III was essentially the same as that of types I and II. Some absorptions were observed to split in type III with the separation of 5–10 cm^{-1}. This is attributed to the intermolecular interaction between two helices in the unit cell. These features of the diffraction pattern and infra-red spectrum indicate that the side chains are well incorporated into the crystalline order. Intra- or intermolecular hydrogen bonds of the side chains are probably formed most effectively.

CONCLUSIONS

The polymorphism of PCLO is of interest from the viewpoint of packing of cylindrical molecules. An α-helical homologue, poly(ε-*N*-carbobenzoxy L-lysine) has simple hexagonal molecular packing, and there are no modifications like those of PCLO[20]. The length and flexibility of the side chain has a serious effect on side-chain interactions and crystal structure. We may summarize the present results as follows.

(1) A new, monoclinic form (type III) of PCLO was found in addition to the (pseudo)hexagonal (type I) and the tetragonal (type II) forms. The lattice and helical parameters were determined by X-ray diffraction technique (*Table 1*).

(2) The structures of types I and II were analysed in the equatorial projection by Fourier synthesis. The structure of type I is extraordinary. The (pseudo)hexagonal unit cell contains two helices, and there is a helix-free space actually filled with side chains.

(3) From the electron-density distribution in the equatorial projection and structure factor calculations, the side-chain conformation is rather disordered and different for types I and II. Urethane groups of the side chains can form intermolecular hydrogen bonds in type I, while the association is intramolecular in type II.

(4) The features of the diffraction pattern indicate that the side chains in type III are well incorporated into the crystalline order, although Fourier analysis was not possible. The existence of 004 and 006 reflections exhibits molecular deformation from the uniform α-helix in the crystal lattice. In most polypeptides having long side chains, the motion of the side chains takes place at about room temperature in the solid state. Therefore, the side-chain region has been believed to be fairly disordered. The formation of type III for PCLO indicates that the side chains are crystallizable although the rate of crystallization is extremely slow. Since the glass-like transition temperature of PCLO associated with the onset of the side-chain motion is about 30°C,[2] the crystallization may proceed during the storage of films at room temperature for a few months. Side-chain crystallization may become possible in other polypeptides by standing films just below the glass-like transition temperature for a long time.

REFERENCES

1 Del Pra, A., Spadon, P. and Valle, G. *Biopolymers* 1973, **12**, 941
2 Sasaki, S., Ban, H. and Uematsu, I. *J. Polym. Sci., Polym. Phys. Edn.* 1983, **21**, 413
3 Elliott, A. in 'Poly-α-Amino Acids' (Ed. G. D. Fasman), Marcel Dekker, New York, 1967, p. 1
4 Fraser, R. D. B. and MacRae, T. P. 'Conformation in Fibrous Proteins', Academic Press, New York, 1973
5 Watanabe, J., Imai, K., Gehani, R. and Uematsu, I. *J. Polym. Sci., Polym. Phys. Edn.* 1981, **19**, 653
6 Sasaki, S., Nakamura, T. and Uematsu, I. *J. Polym. Sci., Polym. Phys. Edn.* 1979, **17**, 825
7 Sasaki, S., Naka, M. and Uematsu, I. *Polym. J.* 1982, **14**, 465
8 Sasaki, S., Watanabe, M. and Uematsu, I. *Rep. Prog. Polym. Phys. Jpn.* 1977, **20**, 613
9 Sasaki, S., Miyamoto, M., Nakamura, T. and Uematsu, I. *Biopolymers* 1978, **27**, 2715
10 Gehani, R., Watanabe, J., Kasuya, S. and Uematsu, I. *Polym. J.* 1980, **12**, 871
11 Sasaki, S., Yasumoto, Y. and Uematsu, I. *Macromolecules* 1981, **14**, 1797
12 Kasuya, S., Sasaki, S., Watanabe, J., Fukuda, Y. and Uematsu, I. *Polym. Bull.* 1982, **7**, 241
13 Watanabe, J., private communication
14 Sasaki, S., unpublished data
15 Luzzati, V., Cesari, M., Spach, G., Masson, F. and Vincent, J. M. *J. Molec. Biol.* 1961, **3**, 566
16 Crick, F. H. C. *Acta Crystallogr.* 1953, **6**, 685, 689
17 Parry, D. A. D. and Elliott, A. *J. Molec. Biol.* 1967, **25**, 1
18 Sasaki, S., Hikata, M., Shiraki, C. and Uematsu, I. *Polym. J.* 1982, **14**, 205
19 Mitsui, Y., Iitaka, Y. and Tsuboi, M. *J. Molec. Biol.* 1967, **24**, 15
20 Yakel, H. L. *Acta Crystallogr.* 1953, **6**, 724